J Agric. Res., 2024, Vol. 62(2):111-119
www.jar.com.pk
Agriculture Department
Government of Punjab

ISSN: 2076-7897 (Online) / ISSN: 0368-1157 (Print)
DOI: https://doi.org/10.58475/2024.62.2.2061

Crossref

AGRI. ENGINEERING

ESTIMATION OF CROP YIELD USING UAV-IMAGES ON BASES OF PLANT HEIGHT AND VEGETATION INDICES

Ahsan Rehman Gill[*1], *Javaria Khan*[2], *Kaniz Fatima*[3] *and Ahmad Nawaz Gill*[4]

[1,2]Visiting Lecturer, University of Agriculture Faisalabad, Toba Campus, [3]Assistant Professor, Principal, Government Associate College for Girls, Faisalabad, [4]Scientific Officer, Oil and Seed Research Institute, Faisalabad.

[*]Corresponding author's email: ahsanrehman41@gmail.com

Article received on: 03/06/2023
Accepted for publication: 18/07/2024

ABSTRACT

Agricultural scientists in agronomy collect crop data such as vegetation index, plant height etc. to gain insight into the overall phenotyping. The purpose of this study was to predict the crop yield using plant height and vegetation indices. Conventional ways of manual ground measurements of the field involve labour and are time-consuming. The research was conducted at Ayub research center Faisalabad in 2022. Fortunately, rapid development in hardware and software of Unmanned Aerial Vehicle (UAV) has provided quite a solution for field crop phenotyping. UAV-photogrammetry is now a trending low-cost and non-destructive approach towards phenotyping. To estimate biomass, we used plant height (PH) derived by subtracting the digital elevation model (DEM) from the digital surface model (DSM) using image-based structure-from-motion (SfM) via UAV imagery. Plant height tends to vary, and this variation can lead us to information on plant health, biomass prediction, yield prediction and plant growth observations as well as response to environmental effects. Before the DSM generation, some image enhancements were also performed that produced different DSMs which we later compared. Alongside the PH we used normalized difference vegetation index (NDVI) with other various vegetation indices (VIs) to calculate the biomass. A sample of ground measurements was also made to evaluate the effectiveness of the PH from UAV images. Finally, we concluded it all by applying regression and correlation on plant height and vegetation indices.

KEYWORDS: Crop yield; yield estimation; image processing; agriculture engineering; phenotyping; Pakistan

INTRODUCTION

Many variables such as irrigation, crop health, disease resistance, quantity of fertilizer used, plant height, etc., evaluate crop yield assessment. Surely these variables play an important role, but to calculate them, it can be quite a difficult job that requires a lot of time and manual groundwork in the field leading to destructive methods that could damage the crop being studied (Yu *et al.*, 2018). Around 30% of the world's territory is covered by forests and still tends to keep 70 to 90 per cent of the world's biomass (FAO and JRC, 2013). To understand biomass in the biosphere, it is essential to have accurate knowledge of the spatial extent, situation, quality and dynamics of trees and plants. To understand their position in the biosphere, accurate knowledge of the spatial extent, situation, quality, and dynamics of trees is essential (Houghton *et al.*, 2009). The collection of such information by fieldwork alone is extremely laborious and in the previous four decades remote sensing methods were made possible, that map to the degree and cohesive structural, multi-spectral and even imposing characteristics of spaces covering the entire planet (Asner and Martin, 2009; DeFries *et al.*, 2010; Hansen *et al.*, 2008; Lefsky *et al.*, 2002; Parker and Russ, 2004; Richardson *et al.*, 2009; R. Zhang *et al.*, 2003). Nevertheless, no single device for remote sensing can capture structural, spectral and forest dynamics at elevated simultaneously spatial resolution (Lefsky and Cohen, 2003). An alternative method is to assess whether the PH estimate could be affected by specific image improvements before DSM generation, just so this model can be further improved. Manual ground measurements are also taken to assess the calculations of plant height acquired by the DSM, followed by a distinction between plant height measurements from the ground and calculated plant height measurements (M Peña *et al.*, 2018). Modern remote sensing technology has a long association with the creation of the camera, which dates to the late 19th century. Camera pictures were originally used on the ground to take intriguing and interesting ways of capturing moments in time and catching something that seemed

truer than drawing or painting and could be caught much faster than drawing or painting. The concept and exercise of remote sensing first arose in the 1980s when it was discovered that it could be possible to take a photo from a viewpoint, such as a different angle or from a building, and attempt to look down at the earth by taking photos using cameras attached to be used. Remote sensing includes the detection and evaluation, by the identification and categorization of radiation from distinct wavelengths that have been recorded or emitted from remote objects. Four basic components in remote sensing for the measurement include the energy source, the target, the remote sensor and finally the transmission path. The energy source recognized commonly as electromagnetic energy is of importance because it acts as the primary way for data transmission from the targeted object to the sensor. It is defined as an electromagnetic spectrum, in which many types of bands represent energy in a spectrum area. The objectives of this study are:

Generate a DSM from the UAV-photogrammetry workflow Calculate the biomass from the multispectral images using NIR VIs Calculate the biomass from the RGB images using RGB VIs

Compare NIR VIs with RGB VIs for better calculations Estimate the biomass and crop yield by applying different statistics among PH and both RGB and Multispectral images.

MATERIALS AND METHODS

The study area is Ayub Agriculture Research Institute fields in Faisalabad in 2022. The institute is known for its accurate measurements of fertilizer, irrigation and the yield obtained from the fields since its sole purpose is research-oriented. It tends to evolve new verities and to develop the technologies for food safety, food security and sustainable generation of exportable surplus, value addition and conservation of natural resources. The temperature in summer ranges from 34°C to 41°C. The experiment field is the central experimental site for spring/summer rapeseed of the Ayub research fields. Scientists working on the study site non-destructively and quantitatively analyze and screen plant phenotypes throughout their life cycle. The experiment consisted of 9 plots that were 3 x 15 m in size. The sowing was done on 5 December 2018. Non-destructive plant height (PH_{ref}) samples were taken in each plot to be compared with CSM-derived PH for reference. Ground control points (GCPs) were distributed evenly across the field, making them easily identifiable in the images. The GCPs were made of 0.3 × 0.3-m laminated cardboard, which was attached to wooden poles that were fixed in the ground. We then measured the position with a differential global positioning system with 0.01-m horizontal and vertical precision. For other research purposes, different fertilizers were applied and soil condition was measured. We did not include those factors in our research.

Fig 1. The field with 9 plots (rows)

Biomass sampling and flight-schedule: Destructive above-ground biomass sampling of 0.04 m^2 was carried out within the sampling areas of each plot. The roots were clipped, samples were cleaned, and stem, leaves and ears were weighed separately on the same day for fresh biomass measurement. For obtaining dry biomass, the samples were then dried at 70 °C for 120 h, and each plant organ was weighed again separately. The values were rescaled to kg per m2. The sampling took place either on the same day or on the day before or after the UAV flights. The biomass sampling area was not excluded from the CSM calculation since it was performed in the last step. Along with biomass we also obtained the yield of the crop from those specific biomass so they could be used at the final estimation stages. For all the flights a manual flight path was from left to right and back to the start to create overlapping. The forward overlap was greater than 90% and the side-lap was greater than 60%. Overlapping helps in creating tie points (matching points). ***CSM, PH and VIs:*** The CSM generation and PH calculation process was divided into two major steps. The first one involved Agisoft Metashape 1.5.3 where the 3D model, DEM and DTM were going to be generated and for the post-processing and analysis part, ArcGIS 10.7 was greatly used. The workflow is presented in Figure 3-4. The individual steps of the data analysis are described below. ***Agisoft metashape Pro:*** The Agisoft Metashape Pro offers a range of outputs from a set of overlapping images such as georeferenced dense point clouds, textured polygonal models, digital elevation models (DEM), digital terrain models

Table 1. Flight schedule and dataset

Type	Date	No. of Images Collected	Point Density (pt./m²)	Ø Image Overlap
UAV (ground model)	5 December 2018	150		
UAV	14 January 2019	160	2878	> 90%
Biomass	14 February 2019			

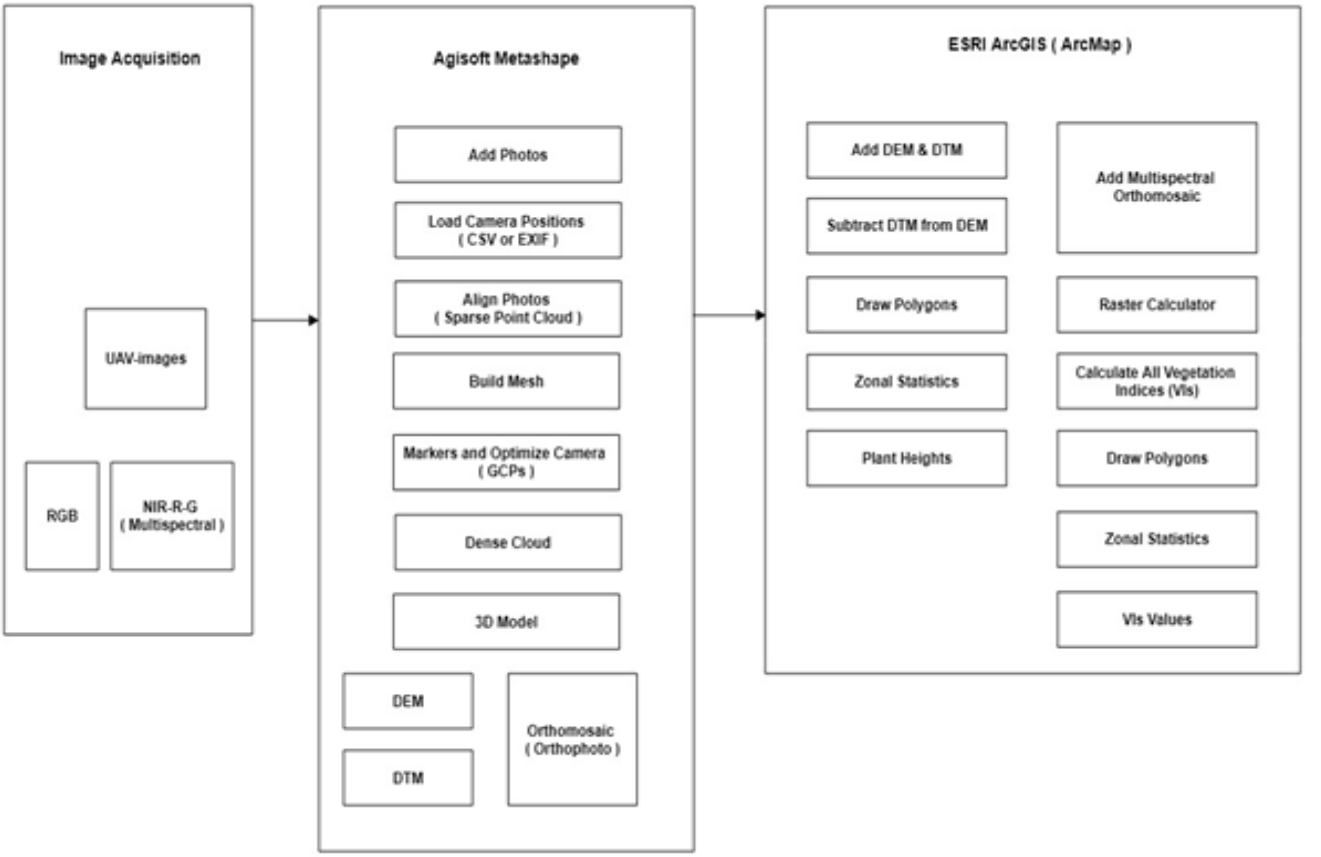

Fig 2. CSM, PH and VIs workflow

(DTM) and orthomosaics. Our workflow is as follows: Add photos and Align them. Generally, the Metashape can create camera positions on its own but If camera positions are available in the form of CSV or EXIF format then they can be loaded by Opening Reference pane using the corresponding command from the View menu. Clicking the import button on the Reference pane toolbar and selecting the file containing camera position information in the Open dialogue. The accuracy should be set to higher. Generic preselection will help in case we don't have camera positions. Reference preselection will be used if the camera positions are known. Key points (tie-points) which are the matching points among the overlapping images can have a limit too. We used the default settings. By aligning photos, we will obtain the sparse point cloud. Which consists of all the matching points in the images that were identified during the alignment process. The more overlapping images we have the more tie-points we will be able to achieve. In our images, we were able to achieve 8,000 points. The next phase involves the placement of the marker on the GCPs that appear on the sparse point cloud and also on the images. They help us in optimizing the camera positions and aligning the entire structure of point clouds. The bounding box that envelops the

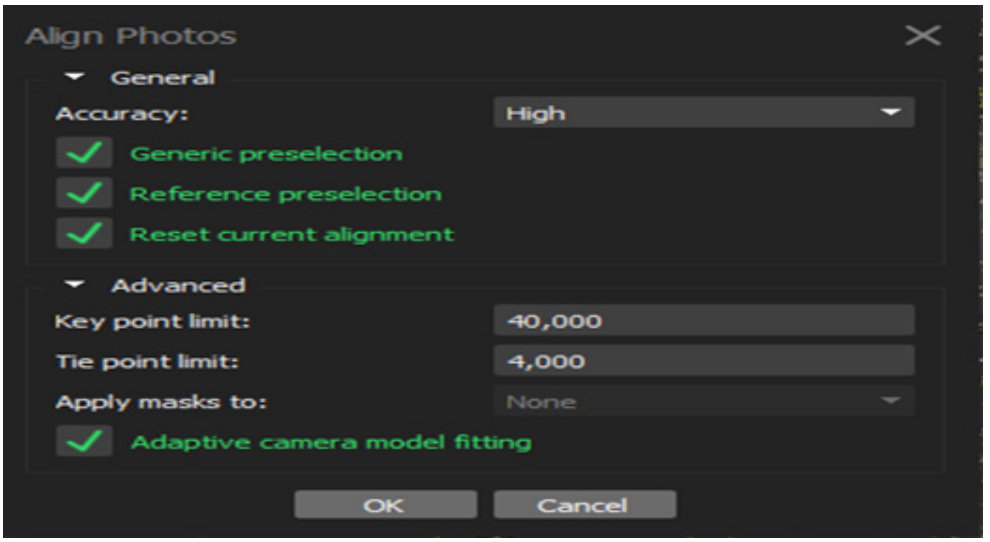

Fig 3. Align photos command in metashape

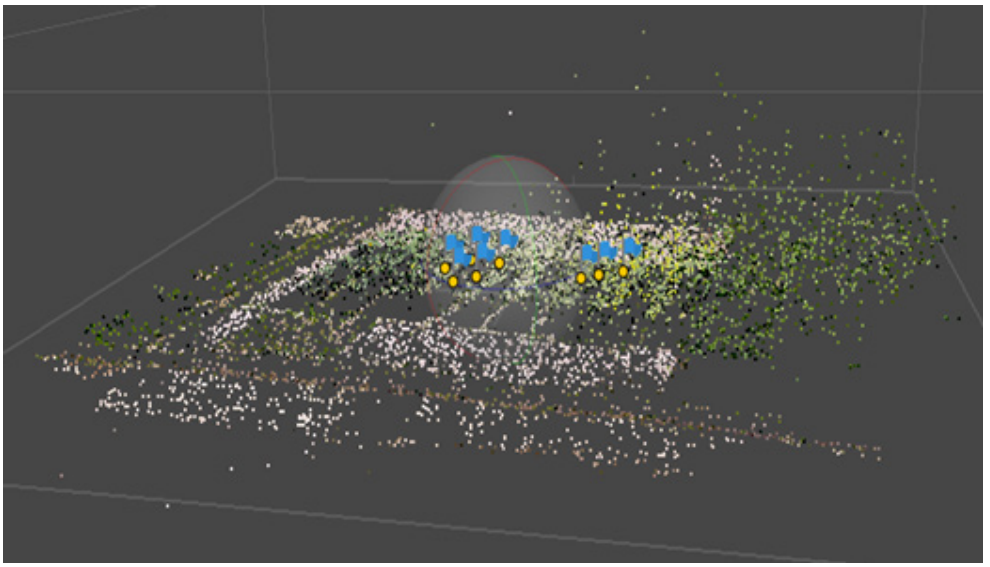

Fig 4. Sparse point cloud

entire sparse point cloud can also be adjusted but we left it as it is since there was no need for changing it. A major step in building the dense cloud is now. Based on the estimated camera positions the program calculates depth information for each camera to be combined into a single dense point cloud. It is to be noted that the term “camera “now refers to images in these sections. The quality depends upon how much depth you want to achieve for your model and how much processing power your system has. We used the ultra-high settings to generate greater results. Depth filtering was left to moderate while we didn’t use the paint colors option since it uses the unnecessary tie-points in the dense cloud point generation. Enabling it won’t help that much since we already achieved a pretty good sparse point cloud in the previous steps

STATISTICAL ANALYSIS

Statistical analysis was performed using SPSS version 29.

RESULTS AND DISCUSSION

Biomass and plant-height

Between 5 December 2018 and 14 January 2019, the test site was flown twice, 50 m above ground level. The first data set was used for the non-vegetable DTM. The fresh biomass obtained from the field and the PH results we calculated are: The correlation shows a strong relationship of 0.827 between the biomass from the field and the PH we

gained from the CSM. The strong relation still doesn't decide whether anyone one of them is dependent upon the other. The Fig 4.1 visually shows an increase among them. A parallel relation is established here. The correlation between PH and biomass was pretty strong and showed the Pearson correlation as 0.827. Without talking about the dependencies it's pretty obvious that the more PH there is the more biomass we can obtain. In this study, the PHCSM represents the mean plant height (PH) of all 0.01-m pixels in a plot. As a result, not only the top of the plant, for example, the ears, is measured, but also the lower parts, like the leaves. Consequently, the detail of PHCSM is higher than PHref, because PHCSM contains more than one pixel per plant and, thus, not only the maximum height. In this context, the method for the PH reference measurements in the field should be discussed. Manual PH measurement is often subjective when the height varies in a plot. The results indicate that measuring 10 randomly chosen single plants does not produce a representative mean of the plot. To solve the problem, a transect could be measured every 0.05 m to better cover the canopy's heterogeneity. Another important factor is the influence of crop movement through wind. From our experience, wind primarily causes a shift in the x-y-direction and does not significantly influence PH measurements. The main constraint of the dataset is the lodging cultivars. A way to mitigate the effect of lodging can be to use the average maximum PH instead of the average mean PH. However, the objective of measuring PH by UAV-based imaging was quite satisfactorily reached. CSMs allow spatial variation in PH and, accordingly, biomass and yield to be identified. This ability is positive in comparison to point-wise sampling where a high number of samples would be needed to allow for a comparable analysis. Even in small-scale field studies of <1 ha, the number of samples that can be collected in a manageable amount of time is limited. The number of samples might influence the comparison of point-wise biomass sampling and spatially measured CSM-derived biomass. In this study, the sampling area did not influence the model development, since it was separated from the measuring area. The PHxGRVI gave R2 of 0.845 and 0.42 for biomass and yield estimation respectively. PHxVARI gave R2 of 0.843 and 0.408. PHxMGRVI gave R2 of 0.851 and 0.433. PHxRGBVI gave 0.823 and 0.464. Lumme *et al.* (2008) used three types of crops with five treatments (n = 15) in six scans during the growing period. Furthermore, no lodging was reported for the comparative studies. Lodging and differences in plant development of the cultivars influence biomass and PH. The results presented here need to be evaluated for field scale studies of multiple years to verify transferability. Several factors, such as water supply and temperature, soil type and status, the type of crop and the phenology, which are commonly considered in crop growth models are not investigated here.

CONCLUSION

In this research, we implemented a straightforward technique for estimating biomass and yield depending on CSM and VIs. First, it was proven to be very

Table 2 Biomass from field and PH calculated from CSM

Row-Id	Biomass (t/ha)	Min-PH (m)	Max-PH (m)	Mean-PH (m)	STD
1	5.320	1.52588E-05	0.691680908	0.263893101	0.170706319
2	6.420	1.52588E-05	0.843032837	0.499090302	0.196481873
3	7.420	1.52588E-05	1.074401855	0.645003475	0.237217262
4	9.230	1.52588E-05	1.087921143	0.725130041	0.212094196
5	8.600	1.52588E-05	1.205490112	0.742636804	0.285318769
6	8.120	1.52588E-05	1.256103516	0.636322	0.308196931
7	10.090	1.52588E-05	1.669387817	1.09076534	0.310128338
8	8.320	1.52588E-05	1.689376831	1.186445006	0.281301712
9	9.640	1.52588E-05	2.581680298	1.198733048	0.302029904

Table 3 Correlation table between biomass and PH

		Biomass	Plant-height
Biomass	Pearson correlation	1	0.827**
	Sig. (2-tailed)		0.006
	N	9	9
Plant-Height	Pearson correlation	0.827**	1
	Sig. (2-tailed)	0.006	
	N	9	9

**. Correlation is significant at the 0.01 level (2-tailed).

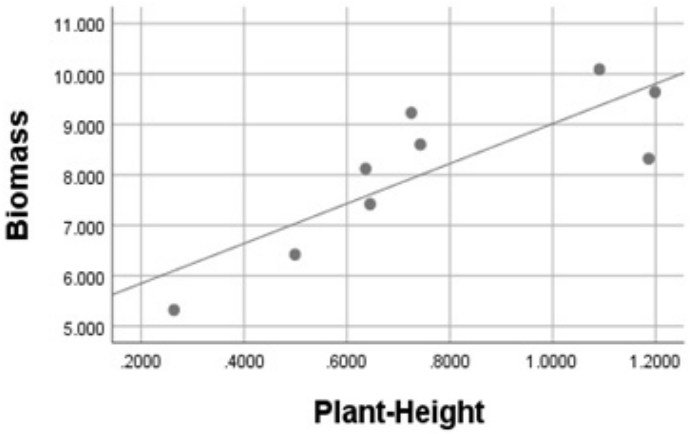

Fig 5. Correlation between biomass and PH

VIs (RGB and multispectral)
The values we calculated from both ortho mosaics are as follows:
Table 4 Visible-VIs values of all the rows

Row-Id	GRVI	VARI	MGRVI	RGBVI
1	0.05135387	0.042295753	0.09787389	0.317147362
2	0.058304224	0.046952518	0.111791918	0.323269973
3	0.043329879	0.034475005	0.083887027	0.280788938
4	0.027067393	0.021693443	0.051791678	0.246333093
5	0.026395633	0.020658799	0.051593059	0.21622712
6	0.02552867	0.02000046	0.049900509	0.200847925
7	0.053860041	0.042100617	0.102123716	0.2488998
8	0.054196505	0.042052066	0.104120653	0.249731757
9	0.042359277	0.032604212	0.082614333	0.23457054

Table 5 Multispectral-VIs values of all the rows

Row-Id	NDVI	SR	SAVI	MSAVI2	OSAVI
1	0.481023646	2.74436136	0.695748759	0.629649993	0.480556671
2	0.531348216	3.079524475	0.766188236	0.684552303	0.530884596
3	0.523701857	3.020658857	0.756306851	0.676577174	0.523242428
4	0.472957346	2.518265283	0.69481369	0.631184547	0.472487551
5	0.455884605	2.350458901	0.675829961	0.616053699	0.455439239
6	0.455298064	2.342231392	0.67554848	0.615680709	0.454853448
7	0.531921534	2.934858196	0.784567254	0.689461469	0.531418029
8	0.521393859	2.835750832	0.770698192	0.6803298	0.520910068
9	0.532432058	2.943092047	0.785249043	0.689911297	0.531933118

Multiple Regression Model

We used the Multiple Linear Regression model for the estimation part. PH x Visible-VIs and PH x Multispectral-VIs were separated into two different models.

Table 6 Biomass and Yield-estimation from PH and Visible-VIs

Row	Biomass	Yield	PHxGRVI		PHxVARI		PHxMGRVI		PHxRGBVI	
			Biomass	Yield	Biomass	Yield	Biomass	Yield	Biomass	Yield
1	5.32	3.01	5.59	3.22	5.57	3.27	5.60	3.20	5.41	3.09
2	6.42	3.76	6.24	3.77	6.23	3.71	6.24	3.79	6.45	3.83
3	7.42	3.80	7.55	3.49	7.57	3.47	7.52	3.49	7.68	3.83
4	9.23	4.40	8.64	3.46	8.61	3.45	8.68	3.48	8.29	3.60
5	8.60	2.70	8.75	3.53	8.74	3.51	8.77	3.56	8.59	3.26
6	8.12	2.90	8.35	3.06	8.39	3.09	8.32	3.06	8.61	2.96
7	10.09	4.90	8.89	4.10	8.92	4.12	8.89	4.10	9.23	4.30
8	8.32	3.40	9.27	4.17	9.31	4.23	9.22	4.13	9.48	4.49
9	9.64	4.70	9.87	4.72	9.80	4.67	9.93	4.75	9.42	4.21

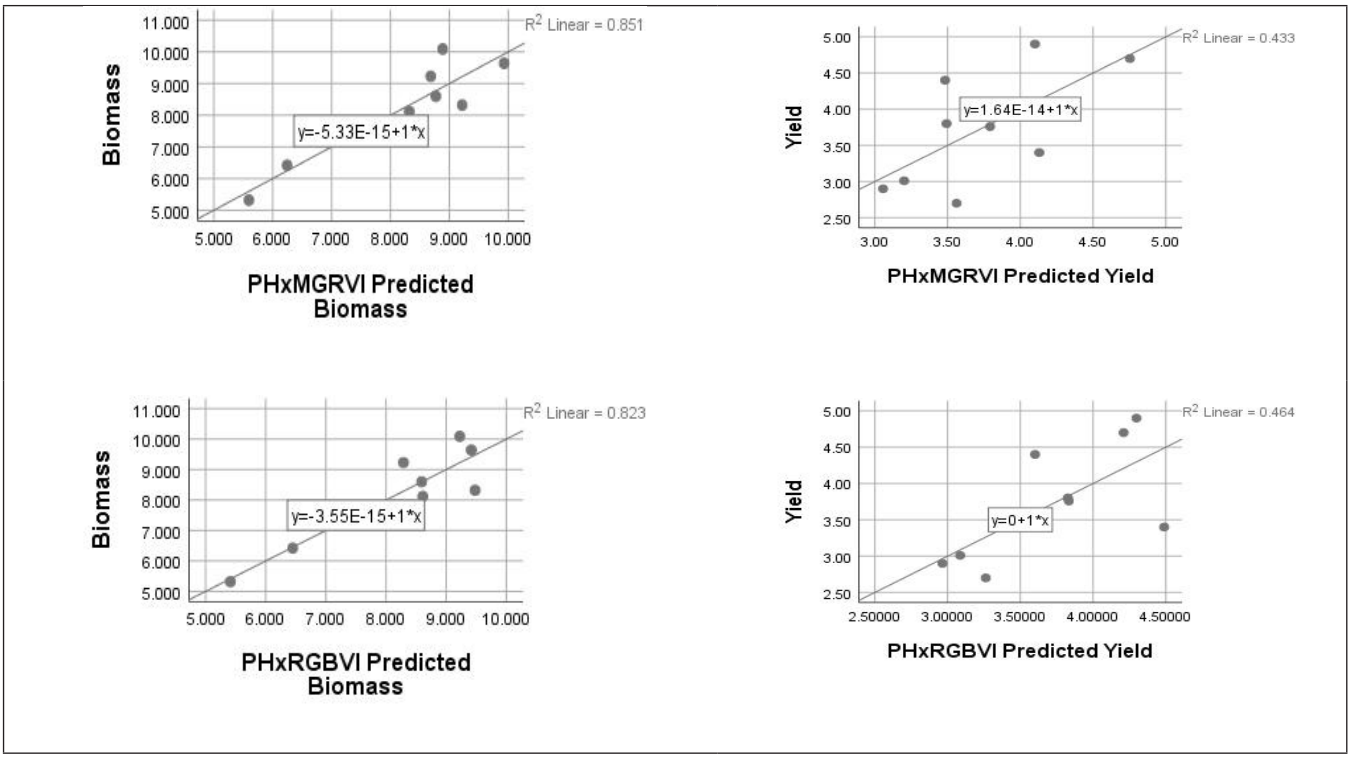

Fig 6. Scatterplots of predicted and actual biomass and yield via PH and VIs

appropriate for deriving barley plant height (PH) from multi-temporal crop ground models (CSMs) with super high accuracy of 1 cm on the ground scale from RGB images from unmanned aerial vehicles. The PH is very precise for various phases of development using elevated-resolution UAV pictures. More detail than point-specific surface measurements is included in the CSMs, which obtain a smaller mean PH per tract. A PH-based approach has been evaluated for the evaluation of plant biomass. Cross-validation has created and evaluated linear models for the estimation of above-ground biomass. The model explains almost 70% of the biomass of rapeseed. Determination coefficients (R2= 0.31–0.72) show that PH from UAV-based images is an appropriate biomass measure. The quality of the model is restricted by accommodating only 1 cultivar and increasing the dispersion of biomass after booting. As far as the literature is concerned, there is only a few research studies that studies the connection between biomass and PH for high-resolution canopy crops. Even fewer surveys discuss the UAV-based imagery and their connection to biomass noticeable band vegetation indicators. UAV-based RGB imaging crop surface models (CSMs) combine both approaches with 3D and spectral information so that alignment problems are avoided, and the processing time is saved. Studies should therefore concentrate on timely techniques such as UAV-based CSMs and orthophotos. RGB imaging UAV-based complies with important elements of RS. The accurate estimate of crop height and biomass generally leads to efficient returns. Considering the above-mentioned population, productivity agriculture is crucial when natural resources become simultaneously sensitive.

REFERENCES

Asner, G. P. and R. E. Martin. 2009. Airborne spectranomics: Mapping canopy chemical and taxonomic diversity in tropical forests. Frontiers in Ecology and the Environment. 7(5): 269–276.

DeFries, R. S., M. C. Hansen, J. R. G. Townshend, A. C. Janetos and T. R. Loveland. 2000. A new global 1-km dataset of percentage tree cover derived from remote sensing. Global Change Biology. 6(2): 247–254.

Houghton, R. A., F. Hall and S. J. Goetz. 2009. Importance of biomass in the global carbon cycle. Journal of Geophysical Research: Biogeosciences. 114(3): 1–13.

Gill,A,R. Nouman,M. Azam,M. 2023. Application of machine learning in estimating ontree yield of citrus fruit. Journal of Agricultural Research. 61(2): 147–153

Hansen, M. C., S. V. Stehman, P. V. Potapov, T. R. Loveland, J. R. G. Townshend, R. S. DeFries,

… C. DiMiceli. 2008. Humid tropical forest clearing from 2000 to 2005 quantified by using multitemporal and multiresolution remotely sensed data. Proceedings of the National Academy of Sciences. 105(27): 9439–9444.

Lefsky, M. A., W. B. Cohen, D. J. Harding, G. G. Parker, S. A. Acker, S. T. Gower, S. Flight. UAV-mapping and ground model generation. Global Ecology and Biogeography. 8(2): 311-314.

M Peña, J., A. I de Castro, J. Torres-Sánchez, D. Andújar, C. San Martín, J. Dorado, F. López-Granados. 2018. Estimating tree height and biomass of a poplar plantation with image-based UAV technology. AIMS Agriculture and Food. 3(3): 313–323

Parker, G. G. and M. E. Russ. 2004. The canopy surface and stand development: Assessing forest canopy structure and complexity with near-surface altimetry. Forest Ecology and Management. 189(3): 307–315.

Richardson, A. D., B. H. Braswell, D. Y. Hollinger, J. P. Jenkins and S. V. Ollinger. 2009. Near-surface remote sensing of spatial and temporal variation in canopy phenology. Ecological Applications. 19(6): 1417–1428.

Yu Zhang, Poching Teng, M. Aono, Y. Shimizu, F. Hosoi and K. omasa. 2018. 3D monitoring for plant growth parameters in field with a single camera by multi-view approach. Journal of Agricultural Meteorology. 74(4): 129–139.

CONTRIBUTION OF AUTHORS

Sr. No.	Author's name	Contribution	Signature
1.	Ahsan Rehman Gill	Conducted the research	
2.	Javaria Khan	Proof read the manuscript	
3.	Kaniz Fatima	Analysed the data	
4.	Ahmad Nawaz Gill	Provided the data